Visualizing fossilization using laser ablation–inductively coupled plasma–mass spectrometry maps of trace elements in Late Cretaceous bones

Alan E. Koenig[1], Raymond R. Rogers[2], and Clive N. Trueman[3]
[1]U.S. Geological Survey, Box 25046, MS-973, Denver Federal Center, Denver, Colorado 80225, USA
[2]Geology Department, Macalester College, Saint Paul, Minnesota 55105, USA
[3]School of Ocean and Earth Science, University of Southampton, SO13 4ZH Southampton, UK

ABSTRACT

Elemental maps generated by laser ablation–inductively coupled plasma–mass spectrometry (LA-ICP-MS) provide a previously unavailable high-resolution visualization of the complex physicochemical conditions operating within individual bones during the early stages of diagenesis and fossilization. A selection of LA-ICP-MS maps of bones collected from the Late Cretaceous of Montana (United States) and Madagascar graphically illustrate diverse paths to recrystallization, and reveal unique insights into geochemical aspects of taphonomic history. Some bones show distinct gradients in concentrations of rare earth elements and uranium, with highest concentrations at external bone margins. Others exhibit more intricate patterns of trace element uptake related to bone histology and its control on the flow paths of pore waters. Patterns of element uptake as revealed by LA-ICP-MS maps can be used to guide sampling strategies, and call into question previous studies that hinge upon localized bulk samples of fossilized bone tissue. LA-ICP-MS maps also allow for comparison of recrystallization rates among fossil bones, and afford a novel approach to identifying bones or regions of bones potentially suitable for extracting intact biogeochemical signals.

INTRODUCTION

Fossilization of bone is a dynamic process controlled by pore-water chemistry, hydrology, temperature, microbiology, and bone architecture. During fossilization the trace element composition of bone is altered, and recent studies (e.g., Metzger et al., 2004; Martin et al., 2005; Trueman et al., 2006; MacFadden et al., 2007) have utilized the uptake of rare earth elements (REEs) to characterize chemical diagenesis in ancient bone. Most previous studies have employed bulk digestion or solution-based techniques such as inductively coupled plasma–mass spectrometry (ICP-MS) to determine the average composition of REE in fossil bone. Here the dynamic nature of fossilization is revealed using laser ablation (LA) ICP-MS to generate high-resolution maps of trace element distributions in a sample of fossil bones collected from sites in the Late Cretaceous of Montana (USA) and Madagascar. Elemental mapping using ion or electron beam microprobes and energy dispersive spectrometry has been used previously to study the fossilization of both vertebrates and invertebrates (e.g., Orr et al., 1998; Goodwin et al., 2007). However, this is the first time that LA-ICP-MS has been used to precisely map the distribution of REEs and other trace elements added to bone post mortem. The LA-ICP-MS elemental maps presented here provide a previously unavailable high-resolution visualization of the complex physicochemical conditions operating within bones during early stages of fossilization.

METHODS AND MATERIALS

LA-ICP-MS permits the investigator to select locations of analyses with great precision. Single point analyses with detection limits for the REE of ~0.1 ppm can be conducted with spot sizes ranging from 5 to 300 µm, and line scans can be targeted across bone tissue at lengths ranging from a few microns to a few centimeters. Two-dimensional elemental maps were constructed using stacked line scans configured as rectangular map areas. Maps were positioned to capture the potential variability in specimens, as estimated by visual inspection (color variation) and previous line scans. Calibration curves were constructed for each mass measured by integrating the signal from the U.S. Geological Survey microanalytical phosphate reference material (MAPS-1), NIST 612 glass reference material, and blank analyses. Each time slice of intensity data along each line scan was converted to concentration using established quantification protocols (Longerich et al., 1996). All calculations utilized a consistent Ca concentration as the internal standard value of known concentration for fossil apatite. The duration of each time slice was converted to distance based on scan speed. After conversion of each time slice to concentration, the lines were stacked into an x-y concentration grid (Woodhead et al., 2007; Becker et al., 2008; Grün et al., 2008). The resulting gridded data for each element were then converted to a false color map using a kriging algorithm and mapping software (Surfer, Golden Software; www.goldensoftware.com).

Fossil bones used for LA-ICP-MS mapping come from three distinct units of Late Cretaceous age. The Montana sample (Fig. 1) consists of three bones derived from a microfossil bonebed (UC-8303) in coastal plain facies of the Campanian Judith River Formation (Rogers, 1998). The Madagascar bones (Fig. 2) were recovered from two units and represent a variety of facies (Rogers et al., 2000, 2007). One bone (ANK101) was mapped from the Ankazomihaboka beds, which consist of cross-bedded sandstones and claystones of fluvial origin. The exact age of the Ankazomihaboka remains unknown, but the unit is underlain by Coniacian basalts dated as ca. 88 Ma old (Storey et al., 1995). Two additional bones were mapped from the Anembalemba Member of the Maastrichtian Maevarano Formation: ANE901 comes from a bonebed intercalated within fluvial deposits in fully terrestrial facies, and ANE951 was recovered from a ravinement bed that caps the unit and separates it from superjacent marine facies.

COMPLEXITIES OF FOSSILIZATION REVEALED

Fossilization of bone can be summarized as hydrolysis of collagen and recrystallization of apatite, where recrystallization refers to growth of apatite crystallites into the space originally occupied by collagen (Trueman and Tuross, 2002). Both the hydroloysis of collagen and the recrystallization of apatite require interaction between bone and pore waters, and trace elements contained in pore waters are readily sorped onto bone mineral surfaces during fossilization (Reynard et al., 1999; Trueman and Tuross, 2002). With continued bone-water exchange, bone will reach equilibrium with pore waters, and elemental concentrations will be similar throughout the

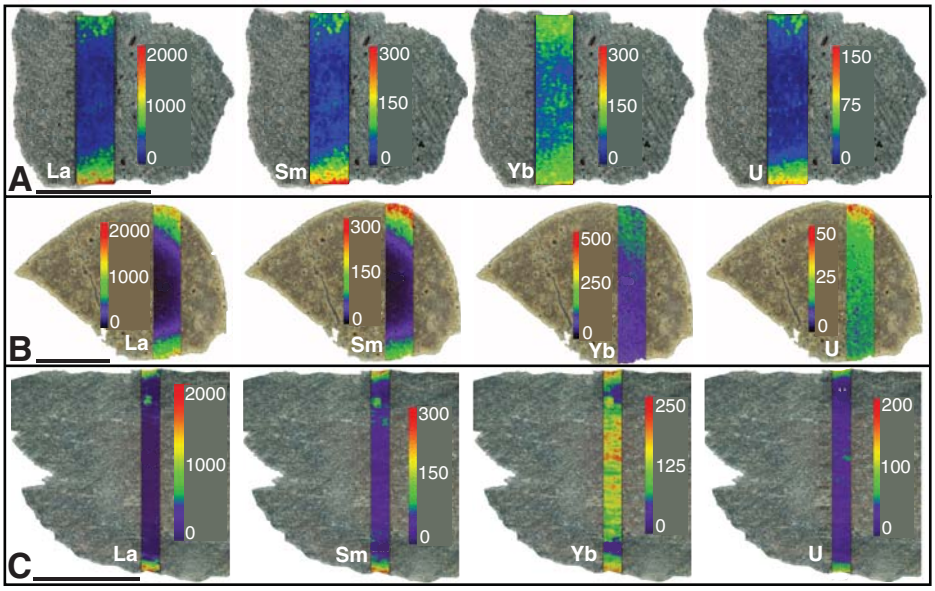

Figure 1. Laser ablation–inductively coupled plasma–mass spectrometry maps of distribution of light (La), middle (Sm), and heavy (Yb) rare earth elements (REEs) and U in bones from bonebed in Cretaceous Judith River Formation, Montana, USA. Numeric scale in parts per million. A, B: Bones show concentration gradients in all elements. C: Bone shows concentration gradients at outer margins and enhanced uptake of heavy REEs within center of bone. Scale bars = 5 mm.

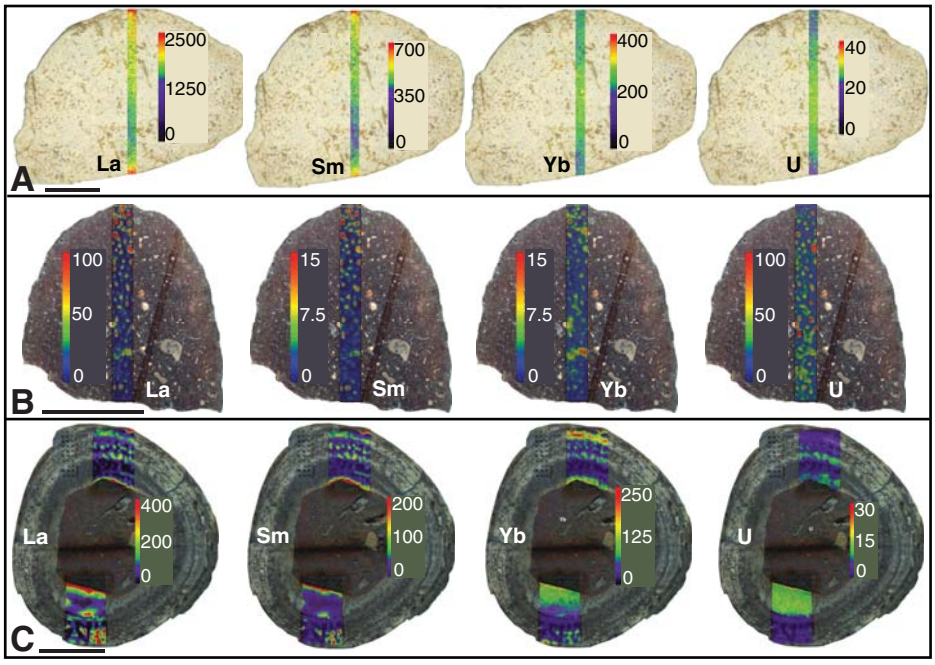

Figure 2. Laser ablation–inductively coupled plasma–mass spectrometry maps of distribution of light (La), middle (Sm), and heavy (Yb) rare earth elements (REEs) and U in bones from Late Cretaceous sediments from Madagascar. Numeric scale in parts per million. A: Bone ANE901 from Anembalemba Member of Maevarano Formation has relatively high concentrations of REEs and U throughout, with shallow concentration gradients in light and middle REEs. B, C: Bones ANE951 (B) from ravinement bed capping the Maevarano Formation, and ANK101 (C) from underlying Ankazomihaboka beds show relatively low total REEs concentrations with distributions indicating transport of REEs via vascular porosity. Highest concentrations are developed within infilled vascular canals and immediately surrounding osteonal tissue. Scale bars = 5 mm.

thickness of the bone (Henderson et al., 1983; Millard and Hedges, 1996; Pike et al., 2002; Trueman et al., 2004). However, the distribution of trace elements in fossil bones is generally not homogeneous, and this presumably reflects variations in diffusive processes within intricately interconnected pore spaces, element-specific variations in the strength of adsorption, and the rate of recrystallization of bone mineral (Henderson et al., 1983; Millard and Hedges, 1996; Janssens et al., 1999; Reynard et al., 1999; Pike et al., 2002; Trueman et al., 2004, Suarez et al., 2007; Kohn, 2008). Recrystallization effectively closes intracrystalline pore spaces, limiting permeability and preventing further diffusion of trace elements within bones. If complete recrystallization occurs before bone has achieved equilibrium, elemental concentration gradients will be preserved that record the distribution of elements in a pre-equilibrium state (Trueman and Tuross, 2002).

Bones from the Judith River Formation (Fig. 1) show distinct gradients in concentrations of REEs and uranium, with highest concentrations generally seen at external bone margins. Concentration gradients show an exponential form consistent with uptake via a diffusion-adsorption mechanism. Concentrations of the light REEs (LREEs, e.g., La) fall more quickly than those of the heavy REEs (HREEs, e.g., Yb), reflecting differences in adsorption coefficients and indicating that trace elements are fractionated from one another during transport and uptake within bone cortex. It is interesting that one bone in the Montana sample (Fig. 1B) shows an asymmetric gradient for U, but not for La or Sm, and this pattern is interpreted to be indicative of redox effects on U uptake (Henderson et al., 1983). Another bone (Fig. 1C) shows both elemental concentration gradients at its margin and elevated concentrations of HREEs in its core. This is interpreted to reflect preferential capture of light and middle REEs via the diffusion-adsorption mechanism at the outer edge and subsequent movement of waters enriched in HREEs within the inner vascular network.

Elemental concentration gradients in Madagascar bones (Fig. 2) differ substantially from the Montana sample. Bone ANE901 (Fig. 2A), recovered from the Anembalemba Member of the Maevarano Formation, displays shallow REE gradients relative to those established for the Judith River fossils, and U concentrations are enriched in the central portions of this bone. Bones from the ravinement bed that caps the Anembalemba Member (ANE951, Fig. 2B) and the underlying Ankazomihaboka beds (ANK101, Fig. 2C) do not exhibit clear concentration gradients. The limited evidence of diffusion and low total REE concentrations in these bones (especially ANE951) could be interpreted to reflect low trace element availability in

external pore waters. However, elevated concentrations of REEs and U are found within infilled central canals of primary and secondary osteons (Figs. 2B and 2C). This indicates that pore waters interacting with these bones contained available dissolved REEs, which in turn suggests that low concentrations of REEs and U are likely the result of reduced interaction between pore waters and bone.

RECONSTRUCTING RECRYSTALLIZATION RATES

Here the slope of preserved concentration gradients is interpreted as a function of the time taken to achieve complete recrystallization, and preexisting quantitative models (Millard and Hedges, 1996; Pike et al., 2002; Trueman et al., 2008) are applied to predict the post mortem uptake and distribution of uranium within bones as a function of time. Using these models and associated estimates of diffusion and adsorption coefficients for uranyl ions in bone, estimates of the minimum time required to produce measured U distributions can be calculated. These estimates of the duration of fossilization are first-order approximations due to uncertainties in environmental concentrations and adsorption coefficients for U species, and are possibly underestimates because the simple version of the diffusion-adsorption (D-A) model adopted here does not consider progressive reduction of either permeability or adsorption coefficients during recrystallization. It is further recognized that the D-A model, although commonly employed to model trace element uptake in fossil bone, is not a unique solution to the question of fossilization, and that other diffusion-limited models may apply (Kohn, 2008). The LA-ICP-MS maps highlighted herein arguably provide a novel means of assessing the nature of diffusive zoning in fossil bones and discriminating among alternative diffusion models.

The D-A model (equation 4 of Millard and Hedges, 1996) was applied to estimate minimum closure rates. Adsorption and partition coefficients for U were estimated as 5×10^{-5} and 1.7×10^{-8} cm^2 s^{-2} respectively (Pike et al., 2002), yielding a D/R (D = diffusion coefficient, R = volumetric equilibrium constant) value of 3.4×10^{-14}. Assigning a single value to these variables assumes a common concentration and speciation of U between burial sites, and constant conditions throughout diagenesis. These assumptions are unlikely to be met in natural systems, and estimated recrystallization rates are thus presented as first approximations. Modeled and measured profiles were compared using least squares regression, and best-fit values of t' (the modeled diffusion gradient) were assigned based on regression statistics. Two bones from UC-8303 yield D-A profiles for both U and Sm. Model curves were fit to profiles and values of t' estimated for U were used to estimate D/R ratios for Sm. Recovered D/R ratios for Sm were 2.6×10^{-14} and 5.7×10^{-14}, respectively, and do not differ significantly from the estimated value for U. Accordingly, Sm profiles were used to estimate minimum closure ages in bones that do not yield U profiles consistent with D-A uptake.

Focusing on the two bones in the Montana sample with relatively symmetric U concentration gradients (Figs. 1A and 1C), minimum rates of recrystallization estimated from D-A models (Millard and Hedges, 1996; Pike et al., 2002) range from ~2.5 to 25 ka. A comparable rate of recrystallization is calculated for the bone with asymmetric U gradients (Fig. 1B) if D-A models are fit to Sm gradients. Shifting to the Madagascar sample, the shallow concentration gradients of ANE901 suggest that this bone underwent relatively prolonged bone-water interaction, and by implication, relatively slow rates of recrystallization. D-A modeling suggests that ~6×10^6 years would be required to reach equilibrium for U assuming a D/R ratio of 3.4×10^{-14}. Given the potential that U concentrations have been affected by redox conditions, and assuming a similar D/R ratio for Sm, a minimum recrystallization time of ~1×10^6 years is calculated for ANE901. Finally, under the premise that the diffusion of REE into bone tissue is mediated by the rate of recrystallization, it is likely that ANE951 and ANK101 recrystallized relatively rapidly. However, given the lack of clear concentration gradients, D-A modeling cannot be applied to these bones, and thus quantitative estimates of recrystallization rates are unavailable.

DISCUSSION AND CONCLUSION

LA-ICP-MS elemental maps provide striking visualizations of the geochemical transition from unaltered bone to fossil bone, and demonstrate with great clarity both the uptake of trace elements into ancient bone tissue and the inherent complexity of diagenesis. For example, some bones (Figs. 1C, 2A, and 2C) show intricate patterns of trace element uptake related to bone histology and its control on the flow paths of pore waters. This complexity must be taken into account when sampling fossil bone tissue for geochemical analyses. Sampling the full thickness of cortex (and thus integrating the total adsorped trace element signal) may be more appropriate than subsampling the outer bone cortex, and findings of previous studies that utilized outer cortical bone to reconstruct relative concentrations of the REEs may need to be reexamined.

Patterns of element uptake as revealed by LA-ICP-MS maps can also be used to address more specific taphonomic questions. Asymmetric profiles (Fig. 1B) arguably serve as graphic geopetal indicators for bioclasts that experienced side-specific microenvironmental conditions during diagenesis (Trueman et al., 2004). Mapped diffusion profiles can also potentially be used to decipher whether breaks in fossil bones occurred before (some semblance of symmetry) or after (marked asymmetry) recrystallization. The potential for exhumation, mixing, and reworking can also be explored by comparing trace element profiles on LA-ICP-MS maps. Diffusion profiles revealed by LA-ICP-MS elemental maps also allow for estimation and comparison of recrystallization rates among fossil bones (and bone-bearing localities). Periods of fossilization for the Montana and Madagascar bones vary between 10^3 and 10^6 years, consistent with previous indirect estimates of fossilization rates (Millard and Hedges, 1996; Janssens et al., 1999; Pike et al., 2002; Trueman et al., 2004, 2008; Kohn and Law, 2006; Kohn, 2008) and with the condition of bone in the archaeological record. Moreover, concentration gradients evident on maps clarify the fact that exquisite morphological and histological preservation does not necessarily correlate with reduced geochemical alteration or even rapid recrystallization. Fragmentary bones from the Ankazomihaboka sandstones (ANK101) and bone pebbles from the ravinement bed that caps the Maevarano Formation (ANE951) apparently underwent relatively rapid recrystallization. In contrast, the bone analyzed from within the Anembalemba Member of the Maevarano Formation (ANE901), which is well known for its exquisite quality of fossil preservation (Rogers, 2005), apparently underwent slower rates of recrystallization and fossilization and greater post mortem alteration of elemental compositions.

This study also highlights the potential for using LA-ICP-MS-generated maps of element distributions as a tool to identify fossils suitable for extracting intact biogeochemical signals. Mean concentrations of Ba and Sr appear to vary with the diffusion profiles of REE, with lower concentrations developed in bones characterized by a poorly developed diffusion gradient (Fig. 3). This in turn suggests that lower concentrations of Ba and Sr characterize bones that experienced relatively faster rates of recrystallization. Bones exhibiting evidence of rapid recrystallization, such as ANE951 in Figure 3, therefore have a greater potential to preserve an in-vivo elemental signal, whereas slowly recrystallizing bones may record a time integrated record of the depositional environment and bone–pore water exchange. Mapped distributions of trace elements thus provide a means to both identify bones likely to yield biological geochemical signals, and better interpret paleoenvironmental or taphonomic information derived from bone chemistry.

Recent work (Asara et al., 2007; Schweitzer et al., 2007) has demonstrated the potential for

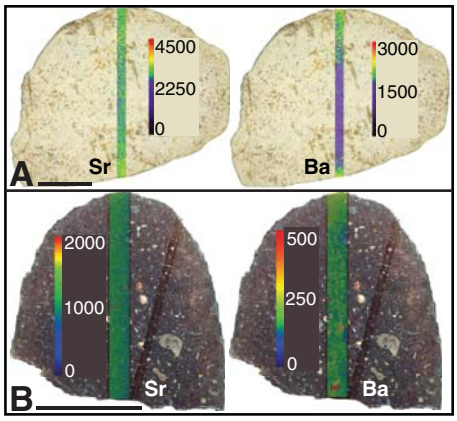

Figure 3. Laser ablation–inductively coupled plasma–mass spectrometry maps of distribution of Sr and Ba in bones from Anembalemba Member of the Maevarano Formation. Numeric scale in parts per million. Sr is distributed uniformly in both bones. Ba exhibits relatively shallow concentration gradient in ANE901 (A) and is more homogenously distributed in ANE951 (B). Lower concentrations of both Sr and Ba are developed in ANE951, and this is consistent with this bone undergoing relatively faster rates of recrystallization. Scale bars = 5 mm.

recovery of intact organic macromolecules from fossil bones. Preservation of organic molecules into deep time presumably requires reduced interaction with pore waters and possibly binding between molecules and mineral surfaces (Schweitzer et al., 2007). In either case, rapid recrystallization is likely to enhance the preservation potential of organic molecules. Given that LA-ICP-MS maps allow for comparison of recrystallization rates among fossil bones, they arguably provide an ideal vehicle for identifying bones or regions of bones most likely to yield intact organic macromolecules.

ACKNOWLEDGMENTS

This research was supported by National Science Foundation grants EAR-0446488 and EAR-0319024 to Rogers and Natural Environment Research Council grant NE/C00390X/1 to Trueman. K. Curry Rogers, P. Emsbo, D. Grandstaff, D. Krause, B. MacFadden, T. Todorov, and an anonymous reviewer provided helpful commentary and discussion.

REFERENCES CITED

Asara, M., Schweitzer, M.H., Freimark, L.M., Phillips, M., and Cantley, L.C., 2007, Protein sequences from Mastodon and *Tyrannosaurus rex* revealed by mass spectrometry: Science, v. 316, p. 280–285, doi: 10.1126/science.1137614.

Becker, J.S., Zoriy, M., Wu, B., Matusch, A., and Becker, J.S., 2008, Imaging of essential and toxic elements in biological tissues by LA-ICP-MS: Journal of Analytical Atomic Spectrometry, v. 23, p. 1275–1280, doi: 10.1039/b805228j.

Goodwin, M.B., Grant, P.G., Bench, G., and Holroyd, P.A., 2007, Elemental composition and diagenetic alteration of dinosaur bone: Distinguishing micron-scale spatial and compositional heterogeneity using PIXE: Palaeogeography, Palaeoclimatology, Palaeoecology, v. 253, p. 458–476, doi: 10.1016/j.palaeo.2007.06.017.

Grün, R., Aubert, M., Joannes-Boyau, R., and Moncel, M.-H., 2008, High resolution analysis of uranium and thorium concentration as well as U-series isotope distributions in a Neanderthal tooth from Payre (Ardèche, France) using laser ablation ICP-MS: Geochimica Cosmochimica Acta, v. 72, p. 5278–5290, doi: 10.1016/j.gca.2008.08.007.

Henderson, P., Marlow, C.A., Molleson, T.I., and Williams, C.T., 1983, Patterns of chemical-change during bone fossilization: Nature, v. 306, p. 358–360, doi: 10.1038/306358a0.

Janssens, K., Vinncze, L., Vekemans, B., Williams, C.T., Radtke, M., Haller, M., and Knöchel, A., 1999, The non-destructive determination of REE in fossilized bone using synchrotron radiation induced K-line X-ray microfluorescence analysis: Fresenius': Journal of Analytical Chemistry, v. 363, p. 413–420, doi: 10.1007/s002160051212.

Kohn, M.J., 2008, Models of diffusion-limited uptake of trace elements in fossils and rates of fossilization: Geochimica et Cosmochimica Acta, v. 72, p. 3758–3770, doi: 10.1016/j.gca.2008.05.045.

Kohn, M.J., and Law, J.M., 2006, Stable isotope composition of fossil bone as a new paleoclimate indicator: Geochimica et Cosmochimica Acta, v. 70, p. 931–946, doi: 10.1016/j.gca.2005.10.023.

Longerich, H., Jackson, S., and Gunther, D., 1996, Laser ablation inductively coupled plasma mass spectrometric transient signal data acquisition and analyte concentration calculation: Journal of Analytical Atomic Spectrometry, v. 11, p. 899–904, doi: 10.1039/ja9961100899.

MacFadden, B.J., Labs-Hochstein, J., Hulbert, R.C., Jr., and Baskin, J.A., 2007, Revised age of the late Neogene terror bird (*Titanis*) in North America during the Great American Interchange: Geology, v. 35, p. 123–126, doi: 10.1130/G23186A.1.

Martin, J.E., Patrick, D., Kihm, A.J., Foit, F.F., and Grandstaff, D.E., 2005, Lithostratigraphy, tephrochronology, and rare earth element geochemistry of fossils at the classical Pleistocene Fossil Lake area, south central Oregon: Journal of Geology, v. 113, p. 139–155, doi: 10.1086/427665.

Metzger, C.A., Terry, D.O., and Grandstaff, D.E., 2004, Effect of paleosol formation on rare earth element signatures in fossil bone: Geology, v. 32, p. 497–500, doi: 10.1130/G20376.1.

Millard, A.R., and Hedges, R.E.M., 1996, A diffusion-adsorption model of uranium uptake by archaeological bone: Geochimica et Cosmochimica Acta, v. 60, p. 2139–2152, doi: 10.1016/0016-7037(96)00050-6.

Orr, P.J., Briggs, D.E.G., and Kearns, S., 1998, Cambrian Burgess Shale animals replicated in clay minerals: Science, v. 281, p. 1173–1175, doi: 10.1126/science.281.5380.1173.

Pike, A.W.G., Hedges, R.E.M., and Van Calstreen, P., 2002, U-series dating of bone using the diffusion-adsorption model: Geochimica et Cosmochimica Acta, v. 66, p. 4273–4286, doi: 10.1016/S0016-7037(02)00997-3.

Reynard, B., Lécuyer, C., and Grandjean, P., 1999, Crystal-chemical controls on rare-earth element concentrations in fossil biogenic apatites and implications for paleoenvironmental reconstructions: Chemical Geology, v. 155, p. 233–241, doi: 10.1016/S0009-2541(98)00169-7.

Rogers, R.R., 1998, Sequence analysis of the Upper Cretaceous Two Medicine and Judith River formations, Montana: Nonmarine response to the Claggett and Bearpaw marine cycles: Journal of Sedimentary Research, v. 68, p. 615–631.

Rogers, R.R., 2005, Fine-grained debris flows and extraordinary vertebrate burials in the Late Cretaceous of Madagascar: Geology, v. 33, p. 297–300, doi: 10.1130/G21036.1.

Rogers, R.R., Hartman, J.H., and Krause, D.W., 2000, Stratigraphic analysis of Upper Cretaceous rocks in the Mahajanga Basin, Madagascar: Implications for ancient and modern faunas: Journal of Geology, v. 108, p. 275–301, doi: 10.1086/314403.

Rogers, R.R., Krause, D.W., Curry Rogers, K., Rasoamiaramanana, A.H., and Rahantarisoa, L., 2007, Paleoenvironment and paleoecology of *Majungasaurus crenatissimus* (Theropoda: Abelisauridae) from the Late Cretaceous of Madagascar: Journal of Vertebrate Paleontology, v. 27, supplement 2, p. 21–31.

Schweitzer, M.H., Wittmeyer, J.L., and Horner, J.R., 2007, Soft tissue and cellular preservation in vertebrate skeletal elements from the Cretaceous to the present: Royal Society of London Proceedings, ser. B, v. 274, p. 183–197.

Storey, M., Mahoney, J.J., Saunders, A.D., Duncan, R.A., Kelley, S.P., and Coffin, M.F., 1995, Timing of hot spot-related volcanism and the breakup of Madagascar and India: Science, v. 267, p. 852–855, doi: 10.1126/science.267.5199.852.

Suarez, C., MacPherson, G., Wolfe, M., Gonzalez, L., and Grandstaff, D., 2007, LAM-ICP-MS analysis of fossil bone: Some unexpected results and implications for interpretation of rare earth elements in fossil bone: Journal of Vertebrate Paleontology, v. 27, supplement 3, p. 154A.

Trueman, C.N., and Tuross, N., 2002, Trace elements in recent and fossil bone apatite: Reviews of Mineralogy and Geochemistry, v. 48, p. 489–521, doi: 10.2138/rmg.2002.48.13.

Trueman, C.N.G., Behrensmeyer, A.K., Tuross, N., and Weiner, S., 2004, Mineralogical and compositional changes in bones exposed on soil surfaces in Amboseli National Park, Kenya: Diagenetic mechanisms and the role of sediment pore fluids: Journal of Archaeological Science, v. 31, p. 721–739, doi: 10.1016/j.jas.2003.11.003.

Trueman, C.N., Behrensmeyer, A.K., Potts, R., and Tuross, N., 2006, High-resolution records of location and stratigraphic provenance from the rare earth element composition of fossil bones: Geochimica et Cosmochimica Acta, v. 70, p. 4343–4355, doi: 10.1016/j.gca.2006.06.1556.

Trueman, C.N., Palmer, M.R., Field, J., Privat, K., Ludgate, N., Chavagnac, V., Eberth, D.A., Cifelli, R., and Rogers, R.R., 2008, Comparing rates of recrystallisation and the potential for preservation of biomolecules from distribution of trace elements in fossil bones: Palevol, v. 7, p. 145–158, doi: 10.1016/j.crpv.2008.02.006.

Woodhead, J., Hellstrom, J., Hergt, J., Greig, A., and Maas, R., 2007, Isotopic and elemental imaging of geological materials by laser ablation inductively coupled plasma mass spectrometry: Journal of Geostandards and Geoanalytical Research, v. 31, p. 331–343.

Manuscript received 6 October 2008
Revised manuscript received 5 January 2009
Manuscript accepted 18 January 2009

Printed in USA